Energy & Environmental Science

Cite this: *Energy Environ. Sci.*, 2011, **4**, 4620

www.rsc.org/ees

PAPER

Silicon thin film solar cells on commercial tiles

Hugo Águas,* Sanjay K. Ram, Andreia Araújo, Diana Gaspar, António Vicente, Sergej A. Filonovich, Elvira Fortunato, Rodrigo Martins* and Isabel Ferreira

Received 6th August 2011, Accepted 19th August 2011
DOI: 10.1039/c1ee02303a

Nanostructured silicon single junction thin film solar cells were deposited on commercial red clay roof tiles with engobe surfaces and earthenware wall tiles with glazed surfaces, with a test area of 24 mm^2. We studied the influence of the type of substrate tile, back contact, buffer layer and SiO_x passivation layer on the optoelectronic performance of the solar cells. Despite the fact that typical micrometre-sized defects on the surfaces of the tiles and the porous nature of the ceramic substrates make deposition of homogeneous thin films on them quite challenging, we have been able to achieve a cell efficiency of 5% and a quantum efficiency of 80% on non-fully optimized cells on commercial tiles. The method is industrially employable utilizing pre-existing plasma-enhanced chemical vapour deposition technologies. The cost-effectiveness and industrial feasibility of the technique are discussed. Our study shows that photovoltaic tiles can combine energy generation with architectural aesthetics leading to significant implications for advancement in building integrated photovoltaics.

1. Introduction

The Sun energy that arrives on Earth accounts for 10 000 times the world energy demand.[1,2] Recent advances in photovoltaic (PV) technology have opened up a multitude of ways to utilize this solar energy, thus providing environmentally friendly sustainable energy solutions. Europe, with Germany (43% of world PV capacity) as the world leader in photovoltaics, has already an installed PV capacity of 30 GW (about 75% of the world's total cumulative PV capacity), which represents 1.2% of Europe's energy demands.[3] Building integrated photovoltaics (BIPV) is one such novel and rapidly growing technology that aims to develop energy-efficient buildings by integrating photovoltaic energy generation into the structure of the building itself. This can be done by PV modules installed on roofs and building façades. It is estimated that 40% of European Union's total electricity demand in 2020 could be met if all suitable roofs and façades were covered with solar panels.[1] The latest data show that more than 1 million BIPV installations already exist worldwide, representing in Europe close to 20% in residences and 75% in commercial and industrial buildings of the total PV capacity installed.[3] Additionally, the use of solar cells in BIPV has allowed the development of a new generation of smart devices, such as the photovoltachromic device[4] that allows the ambient light inside a building to be easily and efficiently controlled. The numbers show that BIPV is clearly a growing market, with an expected growth of 30–40% per year, especially due to political incentives that are being given in Europe. This

CENIMAT/I3N, Departamento de Ciência dos Materiais, Faculdade de Ciências e Tecnologia, FCT, Universidade Nova de Lisboa and CEMOP/UNINOVA, 2829-516 Caparica, Portugal. E-mail: hma@fct.unl.pt; rm@uninova.pt; Fax: +351 21 295 78 10; Tel: +351 21 294 85 64

Broader context

The development of energy-efficient buildings by integrating photovoltaic (PV) modules into the building itself, while keeping good aesthetics and low cost, is one of the major challenges for the PV industry in the near future. Traditional c-Si PV modules present high manufacturing and installation costs as these have to add extra elements to the building structure. As a valid alternative, solar tiles can be much easily integrated in buildings since these can be directly applied in façades and roofs while simultaneously allowing the application of custom cell design patterns that can contribute to a new type of building architecture based on eco-friendly design concepts. This solar cell module concept is then envisaged to allow good architectural integration of the PV modules with buildings, and besides that can be considered as construction components thus reducing considerably their installation costs. Among the several PV technologies available that could be directly integrated with tiles, silicon thin film technology is the most promising one, as it presents good compatibility with the tiles, can be deposited in selected areas, following explicitly selected architecture design patterns and moreover it is an industrial mature technology with a long history of glass module production.

growing trend of BIPV is expected to propagate worldwide, with the USA and Chinese markets already showing great activity in the last couple of years.[3]

In spite of the tremendous growth in PV sector, the energy from PV technology accounts for less than 0.1% of the world energy demand. An important reason for this is the high manufacturing and installation costs of crystalline silicon (c-Si) photovoltaic modules.[5] Among the constraints of BIPV are also the inadequacies in the integration of PV modules with building construction materials, which preclude the availability of PV modules that can be aesthetically and cost-effectively added to buildings.

A ceramic tile with an added functionality of generating energy directly from sunlight is an attractive concept that would correspond to an unexpected and added value to the product and can contribute to a new type of building architecture based on eco-friendly design concepts. Indeed, tiles have been used in façades and roofs of buildings, for aesthetic and insulation purposes for centuries, so they play an important role in urban architecture. A building tile with integrated solar cells, termed here as a solar tile, would serve a double functionality: a conventional function as a barrier against the elements and a non-conventional function as a green source of electricity. Apart from that, additional functionality for ceramic tiles for building integration could be also envisaged by recent works that show the possibility of photocatalytic activity of TiO_2 nanoparticles under visible light in the decomposition of atmospheric pollutants.[6,7] A PV module can be considered as a technical design component of the building architecture, and so it should be possible to consider a part of its cost to belong to the building construction components. Thus, solar tiles could significantly decrease the installation costs as the modules would be applied during the building construction by the contractor, avoiding additional prospective costs with PV panel installation. In fact, the possibility of better aesthetics and building integration and the lack of installation costs make the solar tile an attractive alternative to flexible solar cell laminations on building façades.

Although the concept of solar tiles is interesting and attractive, it is limited by bottlenecks in the manufacturing process. An endeavour to deposit solar cells on building tiles is faced with the challenges of choosing a suitable solar cell material that would be compatible with the porous and rough-surfaced tile substrate, and allow fabrication of transparent or translucent and efficient solar cells capable of withstanding the detrimental effects of atmospheric exposure. In addition, the transferability of the technology from laboratory to industry and the ultimate cost-effectiveness are issues that could be strong deterrents to the commercialization of the PV tiles.

As a result of the above-mentioned difficulties in realizing PV tiles, there have been only a few reports on thin film solar tiles.[8–10] Ref. 8 and 9 describe polycrystalline silicon films deposited by chemical vapour deposition (CVD) on special laboratory alumina and mullite ceramic substrates to produce amorphous/polycrystalline heterojunction cells that exhibited a maximum open circuit voltage of 520 mV with efficiencies below 5%. Ref. 10 presents amorphous silicon (a-Si:H) p–i–n junction cells deposited on commercial porcelain tiles. Commercial tiles are typically more porous than laboratory tiles and have a surface porosity in a size range of tens of microns. In this study, the cells were directly deposited on tiles with indium tin oxide and silver printed back contacts using a p–i–n structure, attaining a maximum efficiency of 4%. Results show a lack of uniformity in cell characteristics within the same tile, with several cells in short circuit. This has been associated with the high surface porosity of the tiles, emphasizing that tiles are not very suitable substrates for a-Si:H solar cell fabrication.

In addition to silicon thin films, the materials that offer the possibility of fabricating solar cells on tiles include thin films of dye-sensitized materials (DSSC),[11] CdTe and $Cu(In,Ga)Se_2$ (CIGS),[5] and organic semiconductors (OPV).[12,13]

DSSC and OPV are attractive new thin film solar cell technologies having potential of offering a low cost product,[14] but stability and efficiency are important issues with them. While OPV solar cells have achieved lab efficiencies of 5–6% for single junction[12,13] and 7% for tandem cells,[12,15,16] rigid substrate silicon solar cells exhibit efficiencies almost twice as high.[17] Recently, Solarmer[18,19] reported OPV efficiencies of 7.9% but scaling up problems of OPV technology persist, leading to module efficiencies of 2 to 3% (ref. 20) for small modules on glass and of 1 to 2% for larger flexible modules,[21,22] which could explain the high cost per peak watt. The best efficiencies achieved with DSSC are also much lower than those reported for thin film silicon solar cells.[14,17] In contrast, silicon thin film technology is a mature technology for efficient and stable solar cells that can be easily adapted by existing industries without the need for new setups.[23–25] The abundance, non-toxicity, low cost and excellent optoelectronic properties of silicon make it an attractive industrial PV material and in spite of being one of the oldest PV materials, it continues to be actively researched for future generation photovoltaics.[26] In addition to these advantages, the high degree of conformability of silicon thin films allows for a better integration with the building tiles with minimal impact on the tile's appearance, design and texture. Si thin films can be deposited on selected areas of the tile yielding partially transparent cells that allow the original surface of the tile to be visible or to follow a design pattern. Si thin films can also be deposited on curved substrates allowing compatibility with traditional curved roof tiles. Further, unlike CdTe and CIGS technologies, environmental toxicity concerns are minimal with silicon thin films for use in buildings.

In this work, we report on the successful fabrication of silicon thin film based solar cells on roof and ceramic tiles with 5% conversion efficiency, following a design pattern over the tiles. We demonstrate the technological approaches that could increase the cell yield in spite of the inherent drawbacks a tile substrate offers, and discuss the feasibility of manufacturing PV tiles in an industrial setup. Since the economic feasibility is also an important concern for the commercialization of the solar tile technology, we have presented the estimates of manufacturing costs of the solar tiles and compared them with glass-based thin film solar modules in an industrial setting, demonstrating the market viability of this technology.

2. Experimental details

Individual doped and undoped (intrinsic) silicon thin films were deposited using a radio frequency plasma enhanced chemical vapour deposition (RF-PECVD) reactor on Corning glass

substrates and characterized using several techniques to obtain their microstructural and optoelectronic properties. A mixture of SiH_4 and H_2 was used to obtain the intrinsic layer, while a further addition of $B(CH_3)_3$ and PH_3 to the same mixture was used to obtain p- and n-layers, respectively. The layers were optimized individually by tuning the deposition parameters to obtain properties suitable for solar cells. After obtaining satisfactory n-, i- and p-layers, the same conditions were used to fabricate n–i–p solar cells on tiles.

A Horiba Jobin Yvon UVISEL spectroscopy ellipsometer (SE) was employed to obtain structural properties and thickness of the silicon films. The SE results were fitted using the Tauc–Lorentz (TL) dispersion model[27] for the bulk material while the surface layer was modelled with the same bulk material mixed with void, according to Bruggeman effective medium approximation (BEMA). The obtained physical parameters are Tauc's optical gap (E_g), physical density (A), broadening term of the Lorentz oscillator (C), and peak transition energy (E_0). The optical gap (E_{op}) of the silicon films was determined by applying the Tauc plot[28] to the spectral variation of the absorption coefficient as a function of the wavelength obtained from UV-Visible spectra of the films. For electrical transport studies, temperature-dependent coplanar dark conductivity (σ_d) of the films was measured under vacuum in a temperature range of 300 K to 380 K leading to the determination of the activation energy E_a and of σ_d at 300 K. The room temperature photoconductivity (σ_{ph}) of the films was measured under AM1.5 illumination conditions.

In order to obtain the best results, the chosen constituent doped and undoped layers of the solar cell were of different microstructural types, having the most suitable optoelectronic properties. The p-type window layer is either amorphous or nanocrystalline silicon (nc-Si:H) material[29,30] or a combination of both, while for the intrinsic layer, a nanostructured material was preferred over completely amorphous Si where nanosized crystallites are dispersed in an amorphous silicon matrix. This type of nanostructured material, often called polymorphous silicon (pm-Si:H), contains less defects than its amorphous counterpart and has better optoelectronic properties with less light-induced degradation.[31–34] For the deposition of pm-Si:H, H_2 diluted SiH_4 is decomposed in plasma in a narrow window of the deposition process at high pressure and high power regime where the small crystals are formed in the plasma and incorporated into the film.[33,35] The PH_3 doped n-layer used in this work was amorphous in nature.

In order to overcome the detrimental effects of surface porosity of tiles, two types of vitreous tiles were used: red clay roof tiles with an engobe surface, hereafter designated as "roof tiles", and earthenware wall tiles with a glazed surface, hereafter designated as "wall tiles". The vitreous surface of these tiles is highly smooth and compact, which is appropriate for thin film deposition and still allows the same architectural integration as other types of tiles. The two types of tiles used in this study were selected after trials with many other varieties of non-vitreous tiles (results not shown here). The roof and wall tiles used in this work were supplied by the Portuguese companies "Coelho da Silva"[36] and "Dominó",[37] respectively.

For the solar cell deposition, 10×10 cm^2 substrates were cut from the commercial tiles and cleaned sequentially with soap water, acetone, isopropanol and deionised water in an ultrasonic bath. After cleaning, the tiles were dried by N_2 and followed by baking at 150 °C. The surfaces of the selected tiles were analysed by optical microscopy and 3D profilometry in order to evaluate the surface roughness and the presence of micro-cavities. An interfacial layer of SiO_x was deposited on the cleaned tiles by the e-beam method using pure SiO_2 pellets. The optimized individual silicon layers were used to fabricate solar cells on the tile surface with the following n–i–p structure (Fig. 1): tile/(back contact)/n-a-Si:H/i-pm-Si:H/p-nc-Si:C:H/p-a-Si:C:H/(front contact). In the n–i–p solar cell structure, the light first passes through the p-layer (window layer). There is a very low absorption of light in the p-layer due to its high band gap (alloying with carbon), low absorption coefficient and very low thickness.

We deposited 12 cells with a defined area of 24 mm^2 on each tile substrate. All the silicon layers were deposited in a single chamber RF-PECVD reactor. In a single chamber reactor, dopant contamination from the reactor walls and electrode surfaces can release freshly deposited dopant-containing molecular species which degrades the performance of the solar cells. To avoid such contamination, we pump down the reactor to get high vacuum immediately after the deposition of the first doped layer. This vacuum was maintained for at least 2 hours to allow slow desorption of the dopant source, which was followed by continuous H_2 flow for 30 min, and finally a short H_2 plasma cleaning to ensure maximum prevention of cross-contamination in the next i-layer deposition.

For the back contact of the solar cells, we test different metals (Al, Ag, Cr and Ti) by evaporating them in vacuum (10^{-6} mbar) using an e-beam system. The transparent conductive oxide (TCO) such as gallium zinc oxide (GZO) was also used for back contact while indium zinc oxide (IZO) was applied for the front contact of the cell.[38] The GZO and IZO layers were deposited by RF magnetron sputtering at room temperature from ceramic targets.[39,40] Finally, the cells were annealed at 150 °C for 1.5 hours in a Nabertherm oven Model L3/11/B170. The I–V curves were measured in a Spire Sun Simulator 240A at AM1.5 (100 mW cm^{-2}) light conditions. Spectral response measurements were performed in the wavelength range of 400 to 800 nm using a Xenon lamp and a DH10 Jobin Yvon monochromator. The substrate surface and cross-sectional device structure of selected samples were analysed by scanning electron microscopy (SEM) in a ZEISS SEM/FIB AURIGA at 2 kV electron energy.

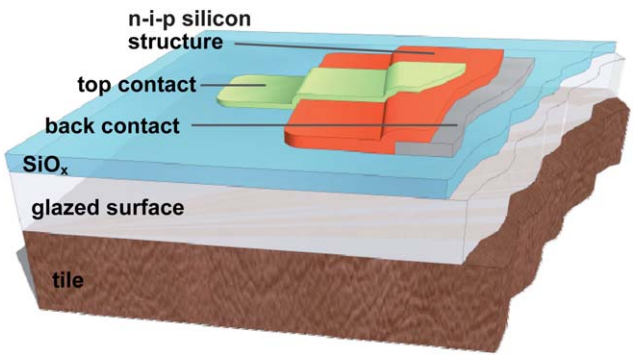

Fig. 1 Schematic view of the silicon thin film solar cell structure on a tile surface.

3. Results and discussion

The typical surface characteristics of the tiles used in this study for solar cell fabrication as studied by using an optical microscope and a 3D profilometer are presented in Fig. 2. The results of the surface analyses show a root mean square (RMS) roughness value of 1.26 μm for the roof tile and 0.19 μm for the wall tile, signifying a higher surface roughness of the roof tile. The micrometre-sized space holes observed on the surface of the roof tile are expected to induce poor cell performance or failure due to the non-uniformity of the layer thickness that can occur at these sites. This is in agreement with the average percentage of working cells attained for each substrate; near 100% for wall tiles and 80–90% for roof tiles. Nevertheless, compared with non-glazed roof tiles that presented a roughness in the order of tens of microns, these tiles have a much smother surface.

Fig. 3 shows the cross-sectional view of the solar cell deposited on the tiles as studied by SEM in order to assess the surface coverage by the thin layers and identify possible causes of failure, such as surface porosity. Fig. 3a clearly shows the buried pores on the bulk and glazed surface layer of the wall tile. While the bulk of the tile shows a rough cleaved surface where many pores can be identified, the glazed layer has less cleavages in the surface with less density of large pores. In non-glazed tiles, these pores can contribute to short circuits in the solar cells deposited on them if present at the surface. The glazed layer drastically reduces these pores on the surface, which can be expected to reduce the detrimental effect of the pores on the cell performance. Fig. 3b shows a higher magnification of the cleavage area close to the surface of a roof tile, where the deposited cell layers and the SiO_x passivation layer are observed. The surface of the tile presents a compact structure, without micrometre-size pores, with excellent surface step coverage by the SiO_x and cell structure layers. These images clearly show that glazed tiles have the preferred surface for thin film deposition compared to regular porcelain stoneware tiles.

Fig. 4 shows the cross-sectional SEM images of cells fabricated with Ti (a) and GZO (b) back contacts. The Ti layer presents the typical granular structure of metals evaporated onto substrates at room temperature, while the IZO and GZO layers both show a much finer grain. The silicon layers (n–i–p) that constitute the solar cell are indistinguishable in the SEM images and appear to be very compact. This is typical of the pm-Si:H (i-layer)[41] which, due to its high compactness, originates some tensile stress that can induce film peeling if deposited directly on a highly smooth surface. In these solar cells, no peeling of the deposited films was observed due to the enhanced adhesion promoted by the SiO_x layer.

Fig. 3 and 4 show that the structure of the SiO_x dielectric layer coating is highly compact and amorphous, which provides an excellent surface coverage of tile for further solar cell layer deposition on top of it. This layer serves both the purposes as an adhesion promoter and ion diffusion blocker thus improving the tile's surface.[42–44]

The microstructural, optical and electrical properties of the individual silicon layers used for the fabrication of the solar cells as studied by SE, UV-Visible spectroscopy and conductivity are presented in Table 1. The results show that the electrical and

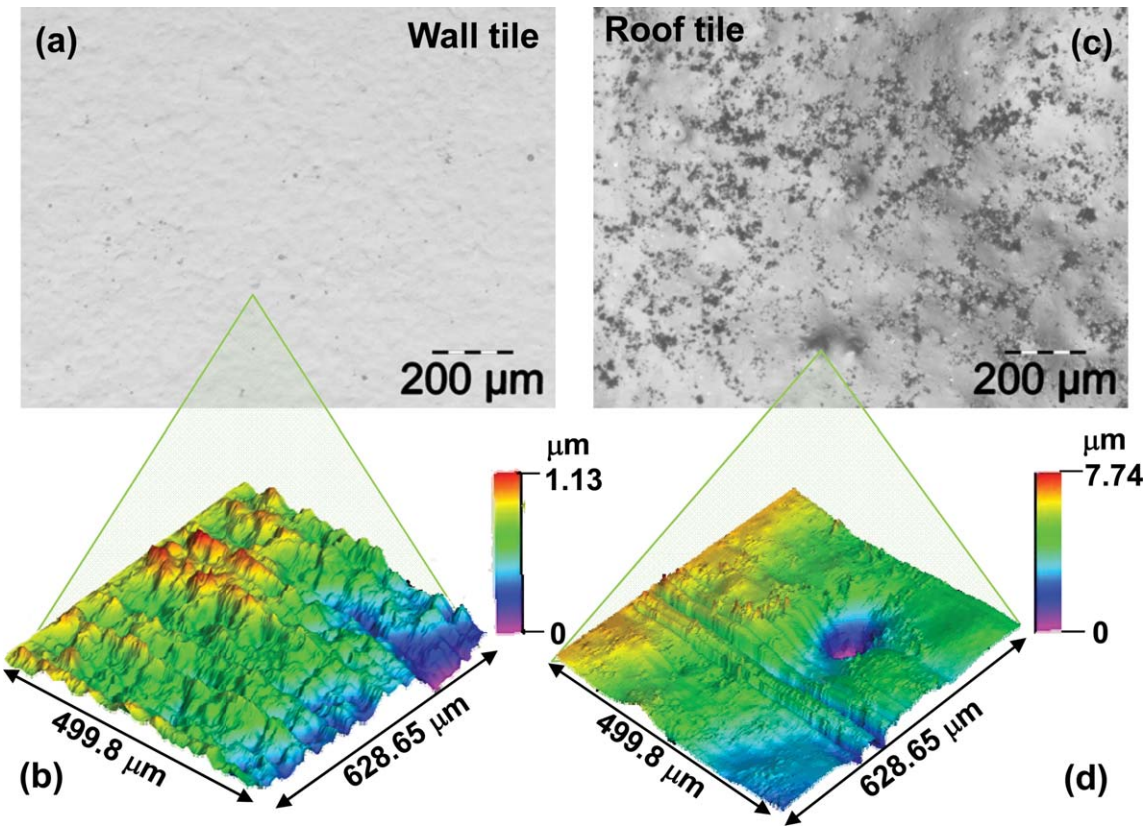

Fig. 2 Optical microscopy images of the (a) wall tile and (c) roof tile, and their respective surface topography (b) and (d) measured by 3D profilometry.

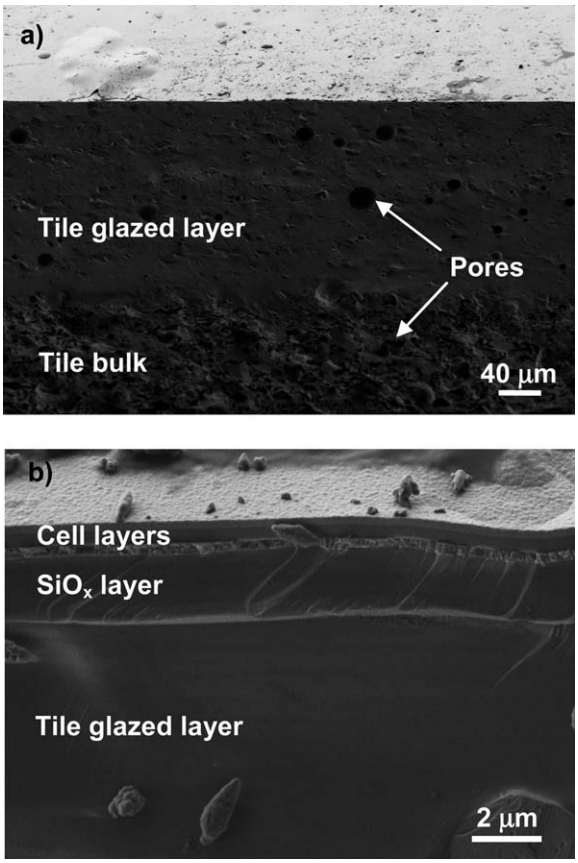

Fig. 3 SEM images of the wall tile (a) and roof tile (b) cross-section with different magnifications.

optical performances of the silicon layers are within the expected range for device grade applications.[34,45,46] The intrinsic pm-Si:H layer has $\sigma_d \cong 6.3 \times 10^{-11}$ $(\Omega\,cm)^{-1}$, a photosensitivity (σ_{ph}/σ_d) of 6.3×10^5, a high SE Tauc–Lorentz parameter, A, of 209 (indicative of compact material) and a low C of 2.13 (indicative of a high short distance order), demonstrating that i-pm-Si:H material has good transport properties and low defect density.[33] The doped layers exhibit a high σ_d and low E_a, particularly the p-nc-Si:C:H with $\sigma_d \approx 0.48$ $(\Omega\,cm)^{-1}$ and $E_a \approx 0.03$ eV. The optoelectronic characteristics of p-layer strongly influence the overall performance of the solar cell since it is the first active layer that light crosses, before being absorbed by the i-layer. Therefore, the p-layer influences the cell's open circuit voltage (V_{oc}) through its optical band-gap (E_{op}), the Fermi level position and the minimum required thickness, *via* the built-in potential and band off set with that one of the i-layer; the short-circuit current density (J_{sc}) by its light absorption coefficient and thickness that determines optical losses at the window layer; recombination losses at both interfaces that depend on the defect density associated with it, affecting the carrier injection efficiency; and the series resistance (R_S) through its conductivity.[47–50]

Keeping this in mind, we tested the cells' performance on the tiles with three different configurations of the window p-layer: an amorphous layer, a nanocrystalline layer and a combination of both. The goal was to determine their influence on the overall properties of solar cells deposited on tiles. The I–V curves of the cells produced with different microstructural types of p-layers and their combinations on roof tiles are presented in Fig. 5.

The results show marked dependence of the solar cell performances on p-type layer characteristics. When the amorphous p-type layer is substituted by a nanocrystalline one, a small decrease in V_{oc} and a large increase in J_{sc} are observed. There is also a slight increase of the slope of the I–V curve near the V_{oc} point, which can be ascribed to a decrease in the R_s. All these differences can be correlated with the microstructural and optoelectronic properties of both the types of p-layers used. The higher E_{op} of the nanocrystalline p-type layer results in a larger band-gap mismatch between the p and i layers at the interface yielding a slight increase of V_{oc}.

On the other hand, the lower absorption coefficient of nanocrystalline silicon and its higher conductivity lead to an increment in J_{sc}. The lower absorption of light in the window layer helps a better collection of the holes from the i-layer. Finally, we combined both the approaches by introducing a nanocrystalline p-layer between the amorphous p-type layer and the i-layer. This also helped to grade the energy bands at the p–i interface and with that to increase simultaneously the V_{oc} while taking the advantages of nc-p layer concerning the collection of carriers in a stacked configuration. As can be seen in Fig. 5, this combination leads to a significant increase of the cells' efficiency from 4 to

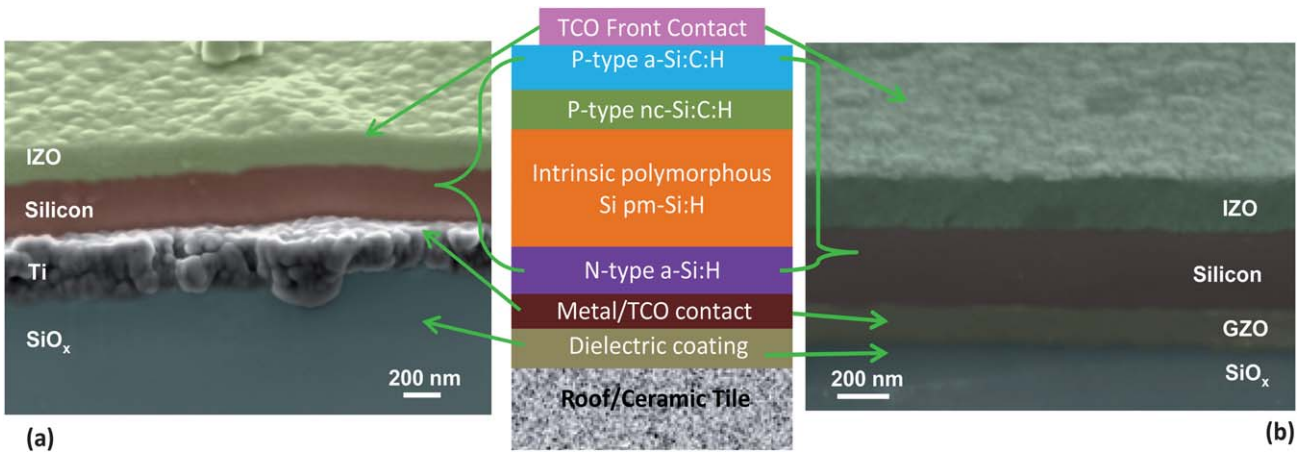

Fig. 4 SEM images showing a cross-section of the solar cell on a roof tile with two different back contacts: Ti (a) and GZO (b).

Table 1 Properties of the silicon layers used in the solar cell fabrication

Conductivity					Spectroscopic ellipsometry		
Layer	E_{op}/eV	σ_d/(Ω cm)$^{-1}$	ΔE/eV	σ_{ph}/(Ω cm)$^{-1}$	A	E_0/eV	C
p-a-Si:C:H	1.84	1.37×10^{-4}	0.29	—	152	3.84	2.83
p-nc-Si:C:H	1.90	0.48	0.03	—	153	4.00	1.89
i-pm-Si:H	1.79	6.3×10^{-11}	1.05	4×10^{-5}	209	3.64	2.13
n-a-Si:H	1.88	1.2×10^{-2}	0.18	—	200	3.64	2.20

5%, where J_{sc} has only slightly decreased from 12.1 mA cm^{-2} to 11.2 mA cm^{-2}, while the V_{oc} reached 0.86 V. Since the intermediate p-nc-Si:C:H layer is nanocrystalline and was made with a very low amount of dopant, the material has less defect densities and can contribute to form high built-in potential for generating a strong electrical field in the active i-layer of Si:H solar cell, resulting in a good buffering effect of improving V_{oc}, and J_{sc}, values compared with single amorphous p layer. However, to minimize absorption losses, we kept the smallest possible thickness of the total p layer (10 nm of p-nc-Si:C:H and 5 nm of p-a-Si:C:H layer), which still maintains both high V_{oc} and high FF. Absorption in the double p-layer leads to slightly lower J_{sc} as can be seen in Fig. 5. Also, the final p-a-Si:C:H layer behaves as a matching layer for defect passivation, improving its interface with the amorphous IZO (TCO) layer.[51] This cell configuration proved to be the most efficient and was thus used in all the solar tile studies presented hereafter.

To evaluate the influence of the type of substrate, several depositions on wall and roof tiles were performed. Systematically, it was found that the cells deposited on roof tiles presented higher efficiency than on the wall tiles, with a difference of nearly 1%.

The *I–V* curves of the best cells obtained with each type of substrates are shown in Fig. 6. These results are consistent with the average of the *I–V* curve characteristics obtained for each type of tiles used over several depositions. The higher current density observed for the roof tile cell can be correlated with its higher surface roughness as previously shown.

On the other hand, the lower V_{oc} of the wall tiles can be explained by the presence of some open glass porosities at the surface of the tile, which causes a local decrease of the cell layer thickness, resulting in modification of the cell's electric field.[52] These results are in agreement with the quantum efficiency spectra presented in the inset of Fig. 6. It can be seen that the maximum responses of the cells occur at 535 nm, with a fast decay for higher wavelengths. This shows that the n–i–p cell structure is not yet fully optimized and there is room for improvement, especially by varying the layers' thickness which can lead to an increase in cell efficiency.

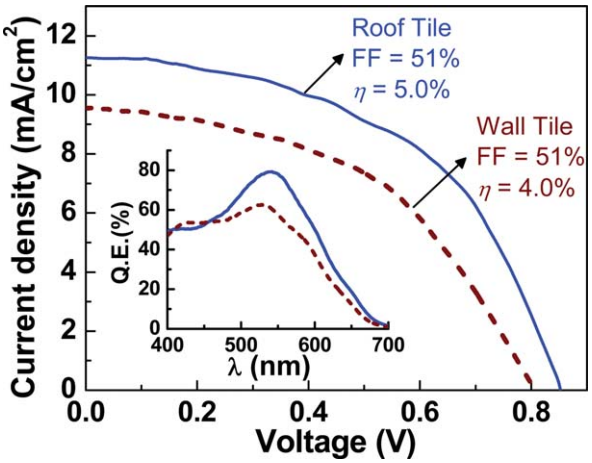

Fig. 6 Comparison of the *I–V* curve and quantum efficiency (inset) of solar cell fabricated on roof and wall tiles.

In order to optimize the cell's back contact, different metals such as Al, Ag, Cr and Ti and one TCO, GZO, were tested. In spite of presenting lower reflectivity than Al and Ag, the best results in terms of cell yield were achieved with Cr and Ti back contacts. The use of Ag and Al caused the majority of the solar cells to be short-circuited. This appears to be a consequence of a partial diffusion of Al and Ag into Si during its deposition, indicating that these metals are less adequate to be used as direct back contacts.

One of the prerequisites for the commercial usability of the solar tiles is that they should be visually attractive for application in building façades. For this, it is desirable that the original colour and texture of the tile remain visible. As an example, Fig. 7 shows the final appearance of the wall and roof tiles with deposited solar cells. The tile holds 12 individual cells with an area of 24 mm^2 each, where the original surface of the tiles can still be observed, as intended.

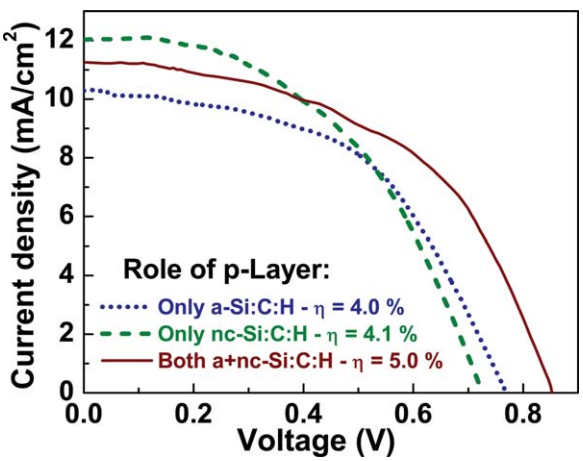

Fig. 5 *I–V* curves of cells obtained using different p-layer configurations, deposited on roof tiles.

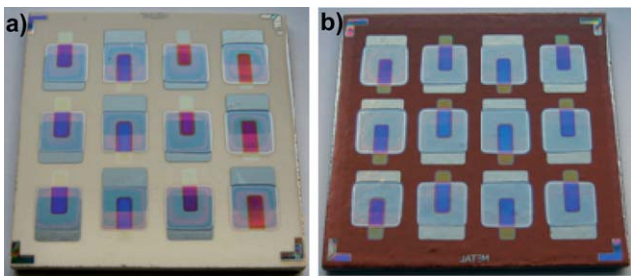

Fig. 7 Pictures of the wall tile (a) and roof tile (b) with the solar cells deposited.

To further increase the visible area of the tiles, the cell back metal contact can be replaced by a TCO material. To prove the feasibility of this concept, GZO was tested as a back contact. This TCO has been successfully applied as a front contact in amorphous silicon p–i–n solar cells.[40] It has a major advantage over indium- and tin-based TCOs, as it is highly resistive against hydrogen plasma induced oxide reduction, which turns the TCO dark and less transparent. This characteristic makes GZO an ideal TCO to be used for deposition of silicon layers from hydrogen diluted silane plasmas, as the ones used here.[53] The *I–V* curve of the resultant solar cell, deposited on a roof tile, is presented in Fig. 8 and compared with the one obtained for the standard Ti back contact. As can be observed, the GZO cell efficiency does not decrease significantly (only 0.2%) when compared with the Ti solar cell. This decrease can be ascribed to a lower reflection of the GZO but if, for example, the substrate had been a bright white tile the results with the GZO could have been even better.

Since the solar cell surface must be protected from the atmosphere, we also investigated the use of a SiO_x layer on the top of the deposited cells as an encapsulation layer. We found that beside that purpose, SiO_x contributes to an increase of the solar cell efficiency, as it is demonstrated by the *I–V* results of the solar cells deposited in wall tiles (Fig. 9). The efficiency increased from 4.0% to 4.3%, as a consequence of a quantum efficiency increment on the region corresponding to the maximum absorption. This result is possibly attributed to an improved refraction index matching between air and cell provided by the SiO_x layer (1.5 for the SiO_x in comparison with 2.1 for the IZO, measured by SE), which reduces the surface light reflection of the cells, besides protecting the solar cell against environment elements (*e.g.*, water vapour and UV light) that may lead to its deterioration. Nonetheless, further investigation on this subject is required as other effects may be involved.

So far, we have successfully demonstrated the fabrication of solar cells on the surface of building tiles and the various methods that can improve the cell efficiency. A photovoltaic building tile is essentially intended for industrial manufacturing to produce an environmentally friendly consumer product. There are significant differences between a laboratory prototype and

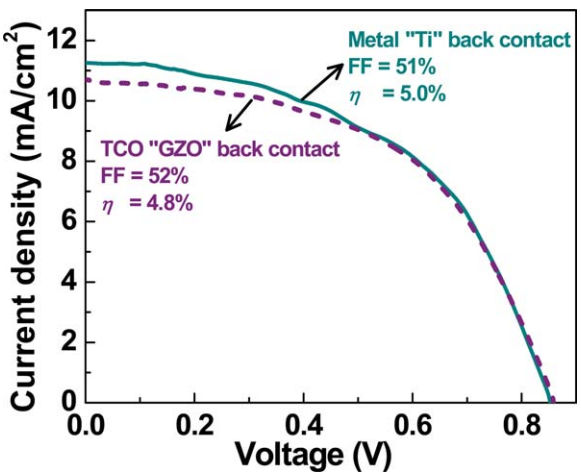

Fig. 8 Influence of the back contact material on the solar cell performance on roof tiles.

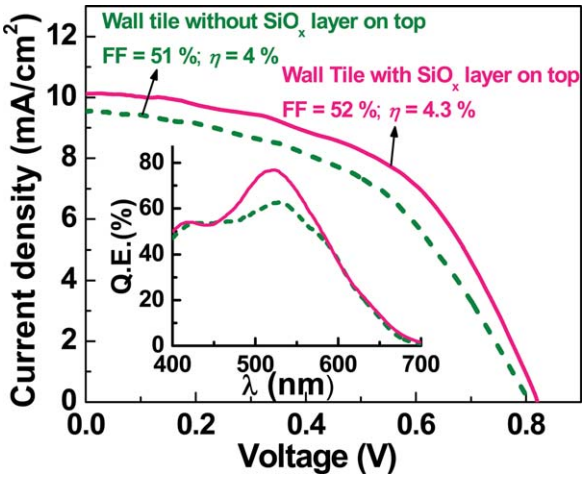

Fig. 9 Effect of the SiO_x passivation layer over a cell in a wall tile in the *I–V* curve and quantum efficiency (inset).

a production design for any device, in terms of the materials, processes and design fidelity. The PV tile will require further refinement in design, and optimization of processes for reducing costs and enhancing efficiency and reliability for a pre-pilot evaluation. However, with the preliminary results, it is possible to envision how the laboratory processes could translate into mass-scale manufacturing processes. In the next subsections, we discuss some of the technical design issues that are important for the usability of the tiles in buildings and compare the steps and costs involved in industrial processing of solar cell modules involving different technologies, including those which would be involved in PV tile manufacturing.

4. Tiles interconnection

An important issue that arises in using tiles integrated with solar cells for building construction is how the electricity generated would be collected. Here we propose a scheme of the electrical interconnections for the solar tile modules described in this article. We envisage three possible products that could use this technology: roof tiles; small 20 × 20 cm^2 to 40 × 40 cm^2 tiles for standard masonry walls; and large 120 × 60 cm^2 tiles for ventilated façades.

For the roof tiles, the proposed connecting systems between adjacent units are similar to a "Lego" connection with male pins and female sockets, with the interconnections placed unobtrusively at the edges of the overlapping tiles to protect them from the elements (Fig. 10b and c). The smaller wall tiles can also have a similar "Lego" type of connectors at the edges of the tiles (Fig. 10d and e), with minor differences in design and will be covered by cement for the installation. The 120 × 60 cm^2 wall tiles are large tiles that are usually used in large buildings with ventilated façades. Due to the large dimension of such solar tile modules and the easy access to the back of the modules provided by the ventilated facade, we propose a system of box connectors with wires in the back of the module.

5. Adaptation to industrial manufacturing process

Many industries, which produce glass-based silicon thin film PV modules, manufacture their own glass or purchase the glass,

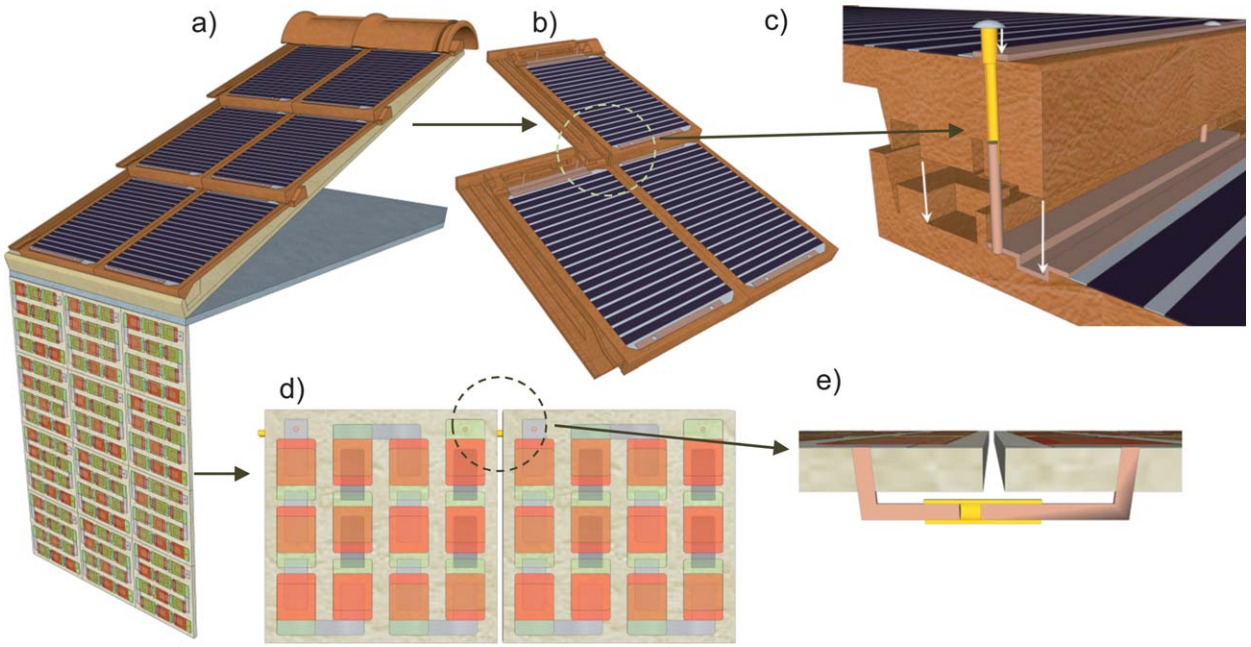

Fig. 10 Schematic concept showing (a) part of a building roof and façade with integrated solar tiles; (b) detail of the roof solar tiles; (c) cut view showing the electrical interconnection detail between roof solar tiles; (d) detail of the wall solar tiles; (e) cut view showing the electrical interconnection detail between the wall solar tiles.

instead of buying TCO-coated glass. The processing of the substrate that is employed in these manufacturing units is similar to what would be required for the Si thin film PV module fabrication on tile substrates. In Fig. 11, we have shown a schematic layout of the processing steps (with time required) which can be used during industrial manufacturing in a classical batch process for production of silicon thin film modules. Thus, briefly, first the tile substrates will need to be cleaned in a proper cleaning station, involving surface brushing followed by a N_2 blow and corona discharge to remove static particles from the surface before starting the deposition processes. SiO_x and SnO_2:F films would be deposited by spray pyrolysis or atmospheric pressure chemical vapour deposition (APCVD).[54,55] This is the deposition process generally used in the PV industry to produce the back contacts of the cells.[56,57]

During the manufacture of the tiles, a highly reflective layer (*e.g.* bright white[59]) can be patterned on the regions where the cells would be deposited, providing additional reflectivity of the tile surface. This would also eliminate the need for metal back reflectors and contribute to lowering of production costs. The substrates are then dry-cleaned and stored in a furnace at 180 °C, ready to start the second process cycle. The time required to complete the first process cycle is estimated to be 44 min. Although the first cycle is shorter than the second one, the substrates can be stored in the furnace for an undetermined time, until they continue to the second process cycle.

The fabrication of n–i–p silicon layers would require industrial PECVD systems using procedures similar to those used for the deposition of p–i–n, single or up to triple junctions on glass substrates, involving amorphous or microcrystalline Si-based structures. The fast deposition technique using very high-frequency (VHF) PECVD systems, which is already employed successfully in many industries,[24] is especially suitable for the PV tiles as it can result in substantial cost reduction. These industrial deposition systems also have load-lock chambers with high vacuum pumping speeds and can deposit on several substrates simultaneously, resulting in a lower module cost.

For the patterning of the solar cells, laser scribing, traditionally used for silicon thin film cell integration, is the best suited method for the solar tiles during industrial manufacturing. The method of screen printing, which is typically used in OPV, is not suitable for the PV tiles due to the possibility of damaging effects of the chemical etching process.[21] The encapsulation of the solar tile modules would be done best with a polymer EVA[60] foil lamination, the same material that is used for OPV and silicon flexible devices.[22,61,62] The second process cycle has an estimated duration of 260 to 300 min, depending on the type of cell structure (single junction amorphous; double junction amorphous; or micromorph) produced, which yields total process times of 304 to 344 min per module. These batch process times correspond to the production of individual modules. Knowing that in industry the PECVD deposition process, the heating stages and the load-lock chambers can handle multiple substrates in parallel, the process batch time for the production of a series of substrates can be estimated to be significantly shorter than that previously mentioned (~70 to 80 min per module). This is a key production point that cannot be directly compared with R2R processes, where continuous processing is used instead of parallel discrete processing. As an example, processing speeds of 1–2 m min^{-1} are now achieved by OPV, R2R processing.[21,63]

5.1 Cost estimation of industrial manufacturing of the Si thin film solar module on tiles

An important consideration for the photovoltaic tile to achieve commercial success is its cost-effectiveness. The infrastructure

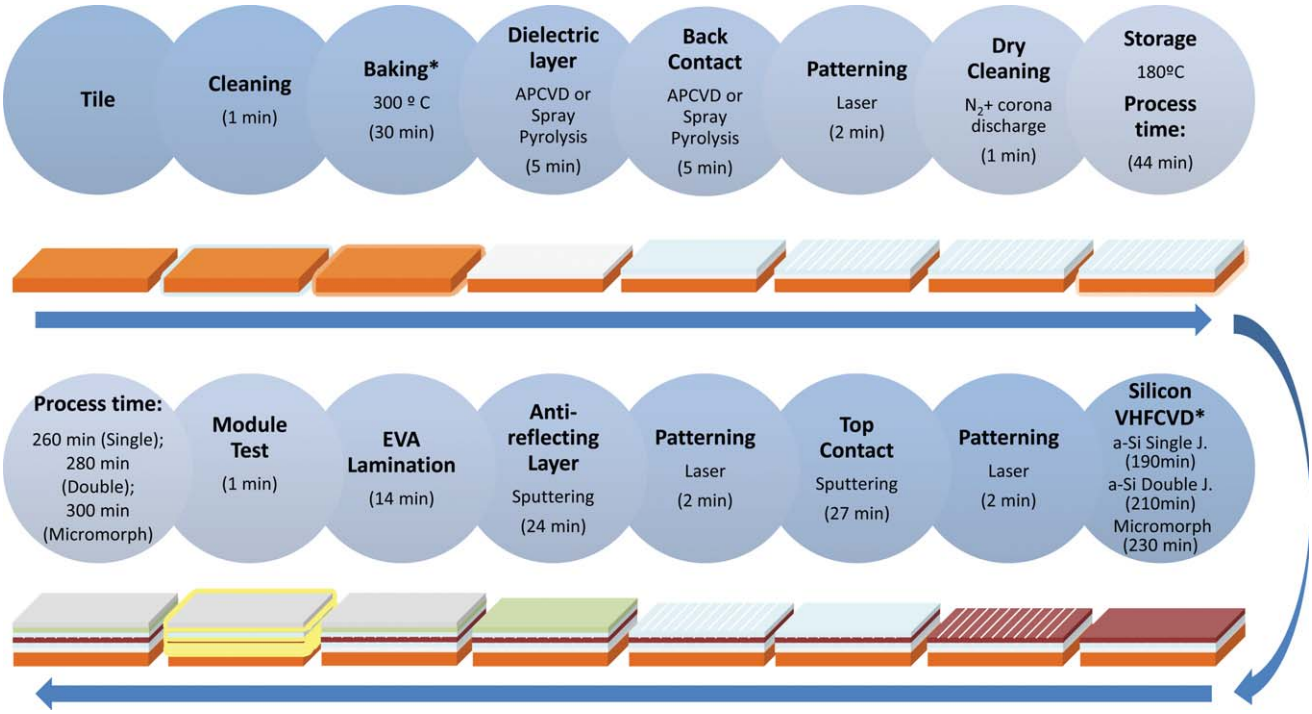

Fig. 11 Solar tiles layout process diagram based on the classical batch process for silicon thin film module production on glass, where load-lock vacuum systems with large diffusion pumps are typically used to achieve low pumping times. In the first process cycle (top), the substrates are cleaned and coated with the protective dielectric layer and back contact and stored in a hot, dry furnace, ready for the second process cycle (bottom), which includes the silicon structure deposition, the top contact and the final encapsulation. The silicon process times were considered according to the final cell structure: a-Si single junction, a-Si double junction, and Micromorph (a-Si/μc-Si) tandem junction. * Typically, these steps use a batch process of 10 simultaneous substrates, so that the time process for each substrate can be estimated by dividing the presented time by 10.

and equipment required for the PV tiles described in this article are the same as what exist in any industry manufacturing thin film silicon solar modules on glass panels, leading to no extra capital costs in terms of manufacturing setup. However, the overall manufacturing process and material costs for the PV tiles, and how they compare to other existing technologies will influence the ultimate economic feasibility of the PV tile technology. In this subsection, we attempt to estimate the manufacturing cost of the PV tiles, and compare it with the manufacturing cost of other technologies, with special consideration to glass-based amorphous silicon solar modules as it is a closely similar technology.

The other commercially available alternatives to PV tiles for similar integration of photovoltaics to building walls are flexible thin film silicon and organic solar cells that can be produced by a roll-to-roll technique. While the roll-to-roll technology uses cheap aluminium and polymer foils as substrates, the price of tiles is not very different from glass. Current production cost for 4 mm glass typically used in thin film Si module fabrication is in the order of \$16 per m^2, while roof tiles are produced at \$14 per m^2 and the large 120×60 cm^2 wall tiles are typically produced at \$52 per m^2. Thus, the roll-to-roll technology has an advantage over the rigid substrate technologies in terms of substrate costs. Table 2 summarises and compares the different technologies in terms of the process steps involved and maximum module efficiency achieved. This will also help us to estimate the production costs involved.

The major manufacturing cost of the thin film PV module depends on the effect of multiple factors, such as manufacturing site (labour and utility costs may vary with the location), material parameters (cost and properties), equipment parameters (speed, cost, and capacity), design parameters (device yield, size, and efficiency) and factory parameters (volume, number of shifts, and automation). The distribution of such costs among these different parameters can be seen in Fig. 12(a) for a 10% efficient Si thin film (amorphous and microcrystalline Si tandem) based solar module on glass panels having an estimated cost of \$0.73 per Wp (in 2011).[64] The material costs, which constitute almost 42% of the total cost, can further be subdivided into other parameters,[65] as shown in Fig. 12(b). In the previous section, we have described the various processing steps involved in the fabrication of the PV tiles and the estimated time consumption involved in each step during volume manufacture of solar modules on tiles in an industrial setup. Combining this information with the cost estimates of the glass-based PV module manufacturing from the literature can yield a fair estimate of the manufacturing cost of the PV tile.

Considering the fact that PV tiles can be manufactured in the existing industries, which are producing glass-based Si thin film PV modules, for the sake of expediency we first estimate the cost of material and other cost factors which can influence the final cost of PV tiles.

The material cost depends significantly on factors like the type of technology being used by the industry, the type of automation and the capacity of manufacturing plant (by volumes). Therefore, the prices of the final module may differ from plant to plant and location to location.

Table 2 Comparative table concerning processing steps for different solar cell module fabrication technologies

Step	Layers	OPV flexible P3TH:PCBM/PEDOT:PSS	Si film flexible p–i–n silicon	Si film on glass p–i–n silicon	Si film on tiles n–i–p silicon
1	Back contact	TCO–APCVD	TCO–APCVD	TCO–APCVD	TCO–APCVD
2	Absorbing	P3TH:PCBM/PEDOT:PSS–R2R slot-die coating	p–i–n silicon–PECVD	p–i–n silicon–PECVD	n–i–p silicon–PECVD
3	Top contact	Silver R2R slot-die coating	ZnO/Al sputtering	ZnO/Al sputtering	ZnO/IZO sputtering
4	Patterning and integration	Photolithography and etching for the back contact	Laser scribing	Laser scribing	Laser scribing or mask pattern
5	Substrate removal	N/A	Chemical etching deeping	N/A	N/A
6	Encapsulation	Polymer film lamination	Polymer film lamination (back and front)	Glass or polymer film lamination	Polymer film lamination
Module efficiency		1–2% (ref. 21 and 22)	5–6% (ref. 58)	7–10% (ref. 23)	5–9% (estimated)

Keeping this in mind, we have considered the two extreme ends of the projected price, where the lower end of the cost corresponds to the most optimized values, while the higher end corresponds to the possible costs incurred in low capacity industrial plants without automation or having lower throughput.

In Table 3, we show the estimated costs ($ per m^2) of various components used in PV tiles. For comparison, we have presented alongside the cost of the components of the glass-based thin film Si PV module[66] on which our estimates are based. To avoid any underestimation of cost for the PV tiles, we have considered the average prices wherever a price range is stated in ref. 66. We have also considered that the cost of processing, energy consumption and maintenance will be somewhat higher in the case of tiles due to the longer duration of pumping and the additional heating time required in the case of tile after the cleaning process, and added 20% extra expenditure in each of these parameters.

While comparing the costs of different components for tiles and glass, it is interesting to note that a few things that are necessary for glass PV modules are not required in the case of tiles. For example, the tiles do not need a back support as they will be installed on a roof or wall directly; nor do they require a front glass support. Hence, the fitting and sealing of these supports will also not be required in tiles, the economic advantage of which is somewhat negated by the higher lamination cost that will be required to better protect the solar cells on the tiles. Therefore, the cost of lamination here is considered to be what is used in the case of flexible solar cells. For the interconnections and electrical contacts, we considered the same price as in ref. 66, but with our simple design concept (Fig. 10) we hope that this cost can be significantly reduced in the future. Thus the estimated material cost comes out to be in the range of $36.80 per m^2 to $147.4 per m^2.

The above estimates include the cost of the tile, which can be actually considered to be a part of the building material. Since the overall manufacturing cost of the PV tile estimated above is comparable to the thin film silicon solar module, which is installed in addition to the building structure, therefore considering the tiles as a part of the building structure leads to further reduction in the manufacturing cost of the solar cell component. Thus, if the cost of the tiles is attributed to the building costs to be borne by the builder, the cost of the solar cell that must be

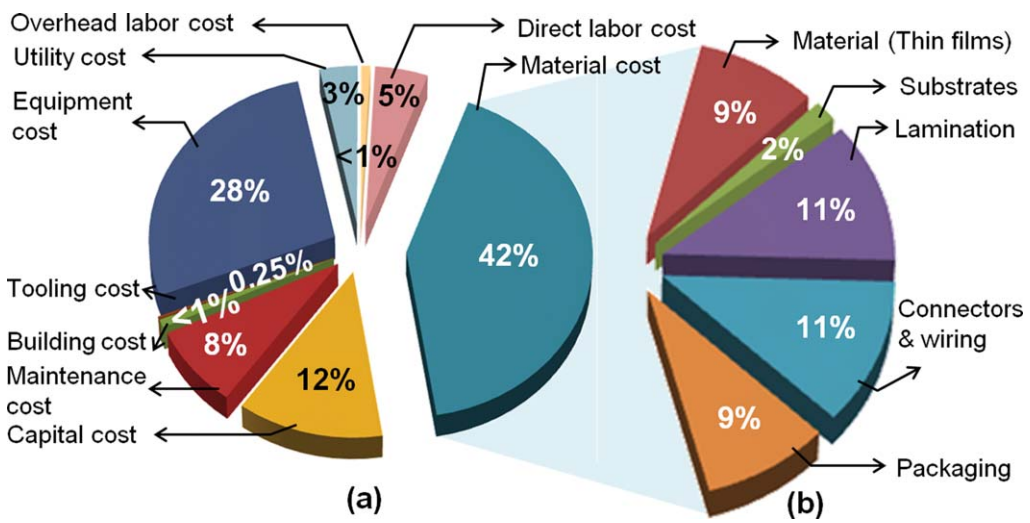

Fig. 12 (a) Cost distribution of thin film amorphous Si (a-Si:H/nc-Si:H) solar module on the glass substrate (with 10% module efficiency with cost $0.73 per Wp in 2011) and (b) further material cost distribution for amorphous Si-based unframed modules.

Table 3 Material cost distribution in thin film Si (single or double junction) solar module on tiles and glass per square metre (cost, $ per m^2)

Material cost distribution in thin film Si (single or double junction) ($ per m^2)					
	Tiles		Glass		
Cost component	Low	High	Low	High	Comment
Substrate	14.00	52.00	6.00	16.00	
Dielectric	2.00	7.00	2.00	7.00	One side TCO coated glass price ($10–17 per m^2)
Antireflecting layers	1.00	5.00	1.00	5.00	
Top contact (TCO)	2.00	5.00	2.00	5.00	
Bottom contact (metal/TCO)	2.00	5.00	2.00	5.00	
Electrical contacts and interconnects	2.90	6.00	2.90	6.00	
Encapsulant (as in the case of flexible SC)	2.90	4.40	1.50	3.00	
Sealant	N/A	N/A	2.90	4.35	
Protecting glass cover	N/A	N/A	5.00	10.00	
Bottom support	N/A	N/A	3.00	9.00	
Edge barrier	N/A	N/A	2.00	6.00	
Thin film Si Material	2.00	30.00	2.00	30.00	High price end also takes into account cost increment due to double junction
Energy[a]	2.00	6.00	1.50	5.00	
Process[a]	3.00	15.00	2.50	12.00	
Maintenance[a]	2.00	5.00	1.50	4.00	
Connection to outside circuit	1.00	2.00	1.00	2.00	
Mounting scheme	0.00	5.00	0.00	5.00	
Total	36.80	147.4	38.80	134.35	
Building material cost in the case of roof or wall material	N/A	N/A	Yes	Yes	Cost of building material will add in the case of separate solar module
Effective total	22.80	95.40	52.80	186.35	

[a] 20% extra costs were added in the case of tiles due to higher consumption of energy, processing, and in maintenance compared with those in the case of glass substrates.

borne by the solar cell manufacturer amounts to $22.80–$95.4 per m^2. For a better visualization of the material cost distributions in the case of the tile based PV module, the data are also presented as pie charts in Fig. 13.

We now come to the estimation of the cost of the PV tile in terms of the electricity generated expressed as $ per Wp, which incorporates efficiency and the yield of the PV tile, allowing a comparison with other PV technologies. This is obtained by dividing the manufacturing cost per square metre as obtained in Table 3 by the output of the same area, which is 1000 Wp m^{-2} times efficiency.[14] The total manufacturing cost includes material cost and other costs, like capital costs, labor costs, *etc.*, similar to what is shown in Fig. 12 for glass-based modules. Thus we convert all the costs in Fig. 13 in terms of $ per m^2 and consider the 'other' costs, such as capital costs, labor costs, *etc.*, to be similar for the PV tile. What differs significantly is the material cost and module efficiency which can affect the total manufacturing cost $ per Wp. The total manufacturing cost of 10% efficient glass-based amorphous silicon solar modules with $0.73 per Wp corresponds to the cost $73 per m^2 (assuming 100% module yield) while material costs and the rest of the costs come out to be $30.66 per m^2 and $42.34 per m^2, respectively. The costs of the different components of the solar cells and processes were collected from various reports in the literature, adjusting for inflation. The material costs of the glass-based thin film silicon solar cells calculated above (~$30) do not include some of the maintenance costs which are necessary to be included when comparing with solar tiles, as they are more relevant in the context of the latter. Therefore, in Table 3, the material cost of the glass-based thin film silicon solar cells is calculated as ~$38, which is not a discrepancy, but a redistribution of the costs to ensure comparability.

Taken as reference the currently achieved efficiency, a projection of costs was done considering a projection scenario (see Fig. 14): from 5% to 9% module efficiency, as realistic future attainable values by modifying the cell architecture to double junction amorphous and micromorph silicon solar cells, for instance.

Based on that, our cost analysis shows that in the present 5% module efficiency situation, the total manufacturing cost of the PV tile modules ranges between $1.66 and $3.98 per Wp. If the cost of the tiles is attributed to the building material cost, then the cost range becomes $1.37–$2.89 per Wp. However, the total manufacturing cost of the PV tile modules can be drastically reduced to $0.92 if it achieves the efficiency barrier of 9% and manufactured in the automated optimized industrial setup. This cost can further be reduced to $0.76 if the cost of the tile is not considered in the PV module manufacturing cost and it is very similar to the cost of 10% micromorph PV module on the glass substrate.

An important consideration for the overall cost analysis of industrial manufacturing is also the energy expenditure involved in the manufacturing process, in terms of life cycle energy analysis. When all the energy input that was spent on producing a PV device is subtracted from the energy it can produce, the net energy content of the device can be estimated, which is especially important for energy generating devices and technologies. The total energy usage based on the Oerlikon process for Si thin film modules was estimated to be 720 MJ m^{-2}, including the capital equipment, materials and gas usages.[67] These numbers can be

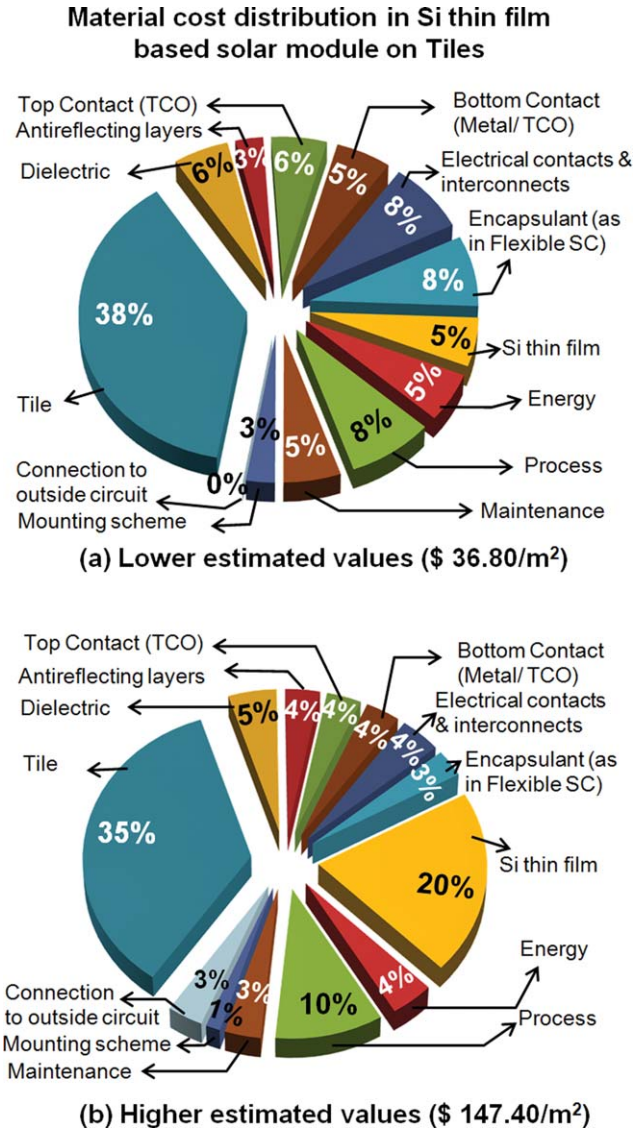

Fig. 13 Material cost ($ per m^2) distribution of thin film amorphous Si (or a-Si:H/nc-Si:H) solar module on the tile substrate: (a) the lower or optimum estimated cost and (b) the possible high end of the price range.

converted to 7.2 MJ per Wp considering 10% module efficiency or 10.3 MJ per Wp considering 7% module efficiency. While similar data for flexible silicon thin film solar cells are unavailable in the literature, still comparing the above data with the data for OPV with reported energy usage for module fabrication in the range of 7 GJ per Wp,[20] Si thin film technology still takes the lead in low cost thin film solar cell module production.

6. Conclusions

Silicon thin film solar cells were deposited on red clay roof tiles with engobe surfaces and earthenware wall tiles with glazed surfaces. Preliminary studies show cell efficiencies of 5% and 4% for the roof and wall tiles, respectively, with yields above 80%.

We have successfully demonstrated that in the n–i–p cell configuration, the use of a p-type nanocrystalline in a stacked configuration leads to a cell efficiency increment and that GZO

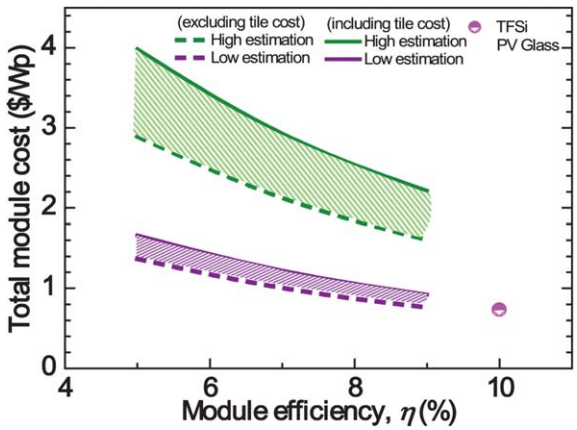

Fig. 14 Learning curves of module cost projection ($ per Wp) as a function of the solar tile module efficiency. In the graph, the dashed lines (green and purple) correspond to the cost projection of the solar tiles when the cost of tiles is attributed to the building material cost, while solid lines (green and purple) correspond to complete cost including tile's cost. In the plot, the data concerning TFSi PV on glass are also shown.[66]

can substitute Ti as cell back contact without significant losses. Quantum efficiency measurements show that the cell's structure is not yet fully optimized, and there is still room for improvement. The use of a SiO_x layer on the bottom and top of the cell can enhance the overall yield and efficiency of the cells. The deposition of a SiO_x layer on the substrate prior to the deposition of cell layers improves their adhesion and can work as a diffusion barrier of contaminating ions from substrate to cell, resulting in increased cell performance. We believe that this is also one of the reasons that contributed to the observed high yield of working cells.

Our estimations of the costs of industrial manufacturing of PV tiles in optimized (lower end) and non-optimized (higher end) conditions show the cost-effectiveness of the solar tiles when compared with the traditional existing technology. To keep the concept of industrial design inherent in our approach to the development of photovoltaic building tiles, aesthetics, environmental ergonomics and usability of the final product have been taken into account at every step. The successful integration of silicon thin film solar cell on the building tiles shows that the tiles can function well as substrate for amorphous silicon thin film-based solar cells, and design components can be added to these solar tiles to create a BIPV component with value-added features. With the potential to combine sustainable energy generation with architectural aesthetics, the PV tiles can add new functionality to the architecture of the future.

Acknowledgements

This work has been financed by the project "SolarTiles (ADI-003380)" from Agência de Inovação with the "Quadro de Referência Estratégico Nacional—Portugal 2007–2013" and from the project "Nanomorph-PTDC/CTM/099719/2008" from the Portuguese "Fundação para a Ciência e a Tecnologia". The authors would like to thank their colleagues Luis Pereira, Tiago Mateus and Rita Branquinho, and all the SolarTiles project partners: Revigrés Lda, J. Coelho da Silva SA, Dominó SA, ADENE, CTCV, De Viris SA, LNEG and Universidade do Minho.

Notes and references

1 *Solar Generation 6: Solar Photovoltaic Electricity Empowering the World*, European Photovoltaic Industry Association—EPIA, 2011.
2 *World Energy Assessment Report: Energy and the Challenge of Sustainability*, United Nations Development Program, United Nations, New York (USA), 2000, pp. 162–163.
3 *Global Market Outlook for Photovoltaics until 2015*, European Photovoltaic Industry Association—EPIA, 2011.
4 A. Cannavale, M. Manca, F. Malara, L. De Marco, R. Cingolani and G. Gigli, *Energy Environ. Sci.*, 2011, **4**, 2567.
5 T. M. Razykov, C. S. Ferekides, D. Morel, E. Stefanakos, H. S. Ullal and H. M. Upadhyaya, *Sol. Energy*, 2011, **85**, 1580–1608.
6 D. Yang, C. Chen, Z. Zheng, H. Liu, E. R. Waclawik, Z. Yan, Y. Huang, H. Zhang, J. Zhao and H. Zhu, *Energy Environ. Sci.*, 2011, **4**, 2279.
7 S. I. In, A. H. Kean, A. Orlov, M. S. Tikhov and R. M. Lambert, *Energy Environ. Sci.*, 2009, **2**, 1277.
8 L. Carnel, I. Gordon, D. Van Gestel, K. Van Nieuwenhuysen, G. Agostinelli, G. Beaucarne and J. Poortmans, *Thin Solid Films*, 2006, **511–512**, 21.
9 A. Slaoui, E. Pihan and A. Focsa, *Sol. Energy Mater. Sol. Cells*, 2006, **90**, 1542.
10 D. Iencinella, E. Centurioni and M. G. Busana, *Sol. Energy Mater. Sol. Cells*, 2009, **93**, 206.
11 L. Gonzalez-Garc, I. Gonzalez-Valls, M. Lira-Cantu, A. Barranco and A. R. Gonzalez-Elipe, *Energy Environ. Sci.*, 2011, **4**, 3426.
12 B. Kippelen and J. L. Brédas, *Energy Environ. Sci.*, 2009, **2**, 251.
13 S. Uchida, J. G. Xue, B. P. Rand and S. R. Forrest, *Appl. Phys. Lett.*, 2004, **84**, 4218.
14 J. Kalowekamo and E. Baker, *Sol. Energy*, 2009, **83**, 1224.
15 S. Sista, Z. Hong, L. M. Chen and Y. Yang, *Energy Environ. Sci.*, 2011, **4**, 1606.
16 J. Y. Kim, K. Lee, N. E. Coates, D. Moses, T. Q. Nguyen, M. Dante and A. J. Heeger, *Science*, 2007, **317**, 222.
17 M. A. Green, K. Emery, Y. Hishikawa and W. Warta, *Prog. Photovoltaics*, 2011, **19**, 84.
18 http://www.solarmer.com.
19 M. K. Siddiki, J. Li, D. Galipeau and Q. Qiao, *Energy Environ. Sci.*, 2010, **3**, 867.
20 N. Espinosa, R. Garçia-Valverde and F. C. Krebs, *Energy Environ. Sci.*, 2011, **4**, 1547–1557.
21 F. C. Krebs, T. Tromholt and M. Jørgensen, *Nanoscale*, 2010, **2**, 873.
22 E. A. G. Hamers, M. N. van den Donker, B. Stannowski, R. Schlatmann and G. J. Jongerden, *Plasma Processes Polym.*, 2007, **4**, 275.
23 Oerlikon press releases, http://www.oerlikon.com/ecomaXL/index.php?site=SOLAR_EN_press_releases, 2011.
24 Fact sheet Thin Fab, www.oerlikon.com/solar/thinfab, 2011.
25 Oerlikon press release, http://www.oerlikon.com/ecomaXL/index.php?site=SOLAR_EN_press_releases_detail&udtx_id=8390, 2011.
26 M. D. Kelzenberg, D. B. Turner-Evans, M. C. Putnam, S. W. Boettcher, R. M. Briggs, J. Yeon Baek, N. S. Lewis and H. A. Atwater, *Energy Environ. Sci.*, 2011, **4**, 866.
27 G. E. Jellison and M. F. Modine, *Appl. Phys. Lett.*, 1996, **69**, 415.
28 J. Tauc, R. Grigorovici and A. Vancu, *Phys. Status Solidi B*, 1970, **15**, 627.
29 S. A. Filonovich, H. Aguas, I. Bernacka-Wojcik, C. Gaspar, M. Vilarigues, L. B. Silva, E. Fortunato and R. Martins, *Vacuum*, 2009, **83**, 1253.
30 H. Águas, S. A. Filonovich, I. Bernacka-Wojcik, E. Fortunato and R. Martins, *J. Nanosci. Nanotechnol.*, 2010, **10**, 2547.
31 P. Roca i Cabarrocas, P. Gay and A. Hadjadj, *J. Vac. Sci. Technol., A*, 1996, **14**, 655.
32 J. Costa, P. Roura, P. Roca i Cabarrocas, G. Viera and E. Bertran, *MRS Online Proc. LIbr.*, 1998, **507**, 499.
33 H. Águas, V. Silva, E. Fortunato, S. Lebib, P. Roca e Cabarrocas, I. Ferreira, L. Guimarães and R. Martins, *Jpn. J. Appl. Phys., Part 1*, 2003, **42**, 4935.
34 L. Raniero, R. Martins, H. Águas, S. Zang, I. Ferreira, L. Pereira, E. Fortunato and L. Boufendi, *Mater. Sci. Forum*, 2004, **455–456**, 532.
35 R. Martins, H. Águas, I. Ferreira, E. Fortunato, S. Lebib, P. Roca i Cabarrocas and L. Guimarães, *Adv. Mater. CVD*, 2003, **9**, 333.
36 http://www.cs-telhas.pt.
37 http://www.domino.pt.
38 E. Fortunato, A. Pimentel, A. Gonçalves, A. Marques and R. Martins, *Thin Solid Films*, 2006, **502**, 104.
39 R. Martins, P. Almeida, P. Barquinha, L. Pereira, A. Pimentel, I. Ferreira and E. Fortunato, *J. Non-Cryst. Solids*, 2006, **352**, 1471.
40 E. Fortunato, L. Raniero, L. Silva, A. Goncalves, A. Pimentel, P. Barquinha, H. Águas, L. Pereira, G. Goncalves, I. Ferreira, E. Elangovan and R. Martins, *Sol. Energy Mater. Sol. Cells*, 2008, **92**, 1605.
41 S. Vignoli, P. Mélinon, B. Masenelli1, P. Roca i Cabarrocas, A. M. Flank and C. Longeaud, *J. Phys.: Condens. Matter*, 2005, **17**, 1279.
42 J. Bregman, J. Gordon, Yoram Shapira, E. Fortunato, R. Martins and L. Guimarães, *J. Vac. Sci. Technol., A*, 1989, **7**, 2628.
43 J. M. M. de Nijs, C. Carvalho, M. Santos and R. Martins, *Appl. Surf. Sci.*, 1991, **52**, 339.
44 C. Nunes de Carvalho, J. M. M. de Nijs, I. Ferreira, E. Fortunato and R. Martins, *MRS Symp. Amorphous Silicon Technology*, 1996, **420**, 861.
45 H. Águas, P. Roca i Cabarrocas, S. Lebib, V. Silva, E. Fortunato and R. Martins, *Thin Solid Films*, 2003, **427**, 6.
46 A. F. I. Morral, R. R. I. Cabarrocas and C. Clerc, *Phys. Rev. B: Condens. Matter Mater. Phys.*, 2004, **69**, 125307.
47 X. Liao, W. Du, X. Yang, H. Povolny, X. Xiang, X. Deng and K. Sun, *J. Non-Cryst. Solids*, 2006, **352**, 1841.
48 P. Kumar, D. Bhusari, D. Grunsky, M. Kupich and B. Schroeder, *Sol. Energy Mater. Sol. Cells*, 2006, **90**, 3345.
49 R. Martins, I. Ferreira, H. Águas, V. Silva, E. Fortunato and L. Guimarães, *Sol. Energy Mater. Sol. Cells*, 2002, **73**, 39.
50 R. Martins, L. Raniero, L. Pereira, D. Costa, H. Águas, S. Pereira, L. Silva, A. Gonçalves, I. Ferreira and E. Fortunato, *Philos. Mag.*, 2009, **89**(28), 2699.
51 L. Raniero, S. Zhang, H. Águas, I. Ferreira, R. Igreja, E. Fortunato and R. Martins, *Thin Solid Films*, 2005, **4487**(1–2), 170.
52 A. Fantoni, M. Vieira and R. Martins, *Sol. Energy Mater. Sol. Cells*, 2002, **73**, 151.
53 L. Raniero, I. Ferreiraa, A. Pimentel, A. Gonçalves, P. Canhola, E. Fortunato and R. Martins, *Thin Solid Films*, 2006, **511–512**, 295–298.
54 Ü. Dagkaldiran, A. Gordijn, F. Finger, H. M. Yates, P. Evans, D. W. Sheel, Z. Remes and M. Vanecek, *Mater. Sci. Eng., B*, 2009, **159–160**, 6.
55 J. Zhang, J. Li, L. Luo and Y. Wo, *J. Alloys Compd.*, 2009, **469**, 535.
56 M. N. van den Donker, A. Gordijn, H. Stiebig, F. Finger, B. Rech, B. Stannowski, R. Bartl, E. A. G. Hamers, R. Schlatmann and G. J. Jongerden, *Sol. Energy Mater. Sol. Cells*, 2007, **91**, 572.
57 Z. Remes, M. Vanecek, H. M. Yates, P. Evans and D. W. Sheel, *Thin Solid Films*, 2009, **517**, 6287.
58 J. K. Rath, Y. Liu, A. Borreman, E. A. G. Hamers, R. Schlatmann, G. J. Jongerden and R. E. I. Schropp, *J. Non-Cryst. Solids*, 2008, **354**, 2381.
59 B. Lipovšek, J. Krč, O. Isabella, M. Zeman and M. Topič, *J. Appl. Phys.*, 2010, **108**, 103115.
60 R. F. M. Lange, Y. Luo, R. Polo and J. Zahnd, *Prog. Photovoltaics*, 2011, **19**, 127.
61 J. K. Rath, Y. Liu, A. Borreman, E. A. G. Hamers, R. Schlatmann, G. J. Jongerden and R. E. I. Schropp, *J. Non-Cryst. Solids*, 2008, **354**, 2381.
62 Helianthos brochure, http://www.nuon.com/nl/Images/Helianthos%20brochure_tcm164-66850.pdf, 2009.
63 F. C. Krebs, J. Fyenbo, D. M. Tanenbaum, S. A. Gevorgyan, R. Andriessen, B. Remoortere, Y. Galagan and M. Jørgensen, *Energy Environ.Sci.*, 2011, DOI: 10.1039/c1ee01891d.
64 Private communication from D. Ginley, Process Technology and Advanced Concepts group, NREL, USA.
65 Technology and market challenges to mainstream thin-film photovoltaic modules and applications by R. Arya, http://www.nrel.gov/pv/thin_film/docs/rajeewa_arya_2004_thin_film_overview.pdf.
66 J. E. Trancik and K. Zweibel, *Proceedings of the World Conference on Photovoltaic Energy Conversion, IEEE WCPEC*, 2006, **vol. 4**(2), p. 2490.
67 R. van der Meulen and E. Alsema, *Prog. Photovoltaics*, 2011, **19**, 453.

